Binary Signal Transmission in Nonlinear Sensors: Stochastic Resonance and Human Hand Balance

Fabing Duan, Lingling Duan, François Chapeau-Blondeau, Yuhao Ren, and Derek Abbott

Many sensors exhibit nonlinear characteristics [1]–[5] and are deployed in noisy environments [1]–[7]. In terms of device design and forming standards, this is a challenging area. However, it also presents opportunities for non-conventional signal processing methods based on stochastic resonance that have been shown to be of benefit for individual nonlinear sensors [1]–[7], sensor arrays [3]–[10], sensor networks [3], [8], [11], and even portable devices for people with reduced sensory capacity [12]–[14]. The most fascinating property of stochastic resonance is that nonlinear sensors connected in parallel or in a network yield improved performance over that achieved by using individual sensors [1]–[10]. Studies in stochastic resonance have led to evidence of noise-enhanced signal transmission and processing in nonlinear sensors, and noise can be exploited in the design of engineered devices [2]–[7], [10] and biological systems [1], [11]–[13]. This paper studies noise-enhanced signal transmission and processing in nonlinear sensors and also exploits the positive role of noise in the design of engineered devices that enhance the sensitivity of hand movements.

From a Single Sensor to a Sensor Array

In order to elucidate interesting aspects of stochastic resonance, we first consider binary signal transmission in sensor arrays with the help of artificially added noise, as shown in Fig. 1. The binary information is modulated as the waveform signal $s(n)$ that is corrupted by the channel noise $\xi(n)$, yielding the input $x(n) = s(n) + \xi(n)$ of the sensor array. We here encounter a dilemma: the type of noise $\xi(n)$ may have a large deviation, and the available sensors are not necessarily optimized to the noise, while the optimal sensors derived by the Neyman-Pearson criterion or the criterion of minimum probability of error may be out of reach as either too complex or too costly. An interesting option is to artificially add noise components $\eta_m(n)$ into an array of non-ideal sensors, delivering the signals $y_m(n)$ ($m = 1,2,\ldots,M$)) to deal with this dilemma, as shown in Fig. 1.

The information-carrying digits 0 and 1 are modulated as the pulse-amplitude modulation waveforms $s_0(n) = -A$ and $s_1(n) = +A$ with equal probabilities, respectively. Assume the environmental noise $\xi(n)$ is Gaussian distributed with zero mean and standard deviation σ_ξ, and the sensors are binary quantizers with input-output characteristics:

$$y_m(n) = \begin{cases} 1, & x(n) + \eta_m(n) \geq \gamma, \\ 0, & x(n) + \eta_m(n) < \gamma, \end{cases} \tag{1}$$

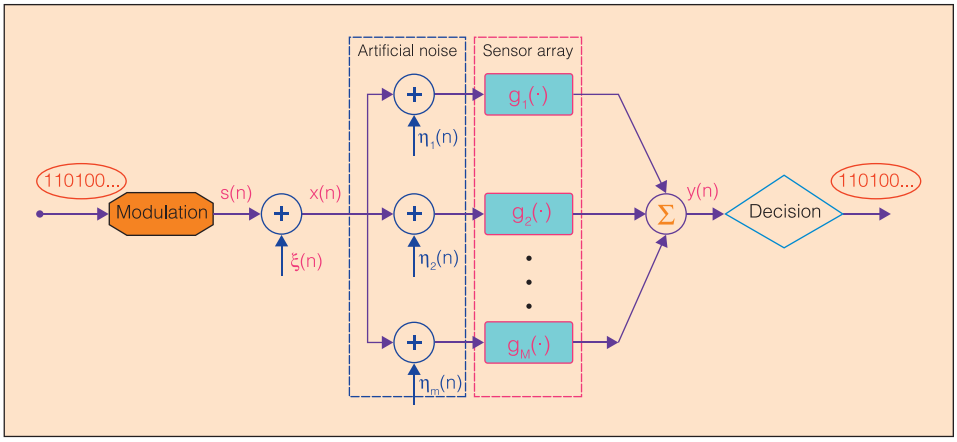

Fig. 1. A schematic diagram of binary signal transmission in a sensor array.

This work is sponsored by the National Natural Science Foundation of China (No. 61573202).

1094-6969/20/$25.00©2020IEEE

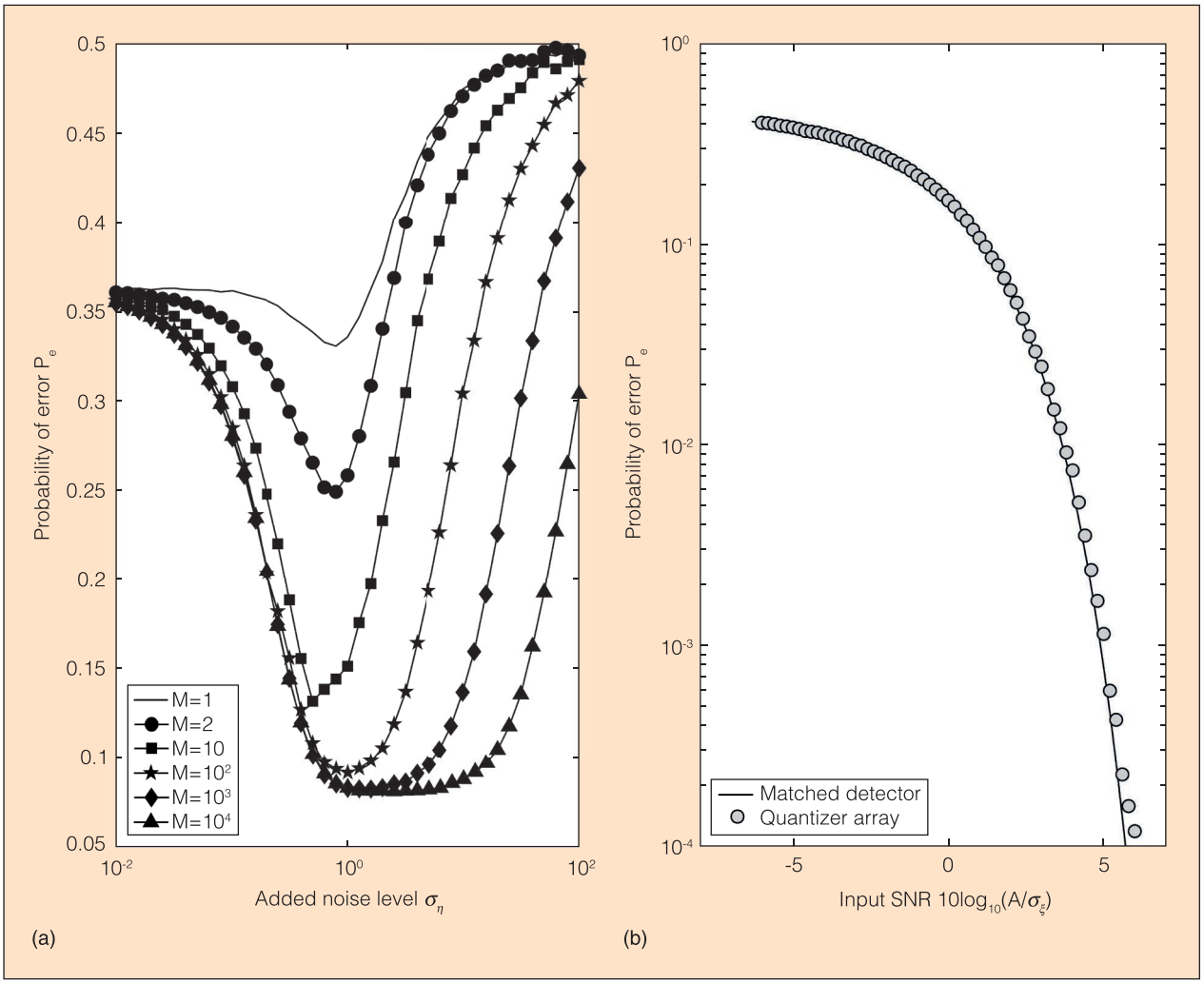

Fig. 2. Probabilities of error versus: (a) the added noise level in binary quantizer arrays of size M, and (b) the input SNR for the matched detector and the quantizer array.

and the threshold γ[1]–[3]. Under this circumstance, the sensor input $x(n) + \eta_m(n)$ will excite the quantizer with the probability $p_i = \text{Prob}(y_m = 1) = 1 - F_\xi(\gamma - s_i)$, where F_ξ is the cumulative distribution of the noise ξ. For a sufficiently large number M, the sum $y = \sum_{m=1}^{M} y_m$ of outputs of m quantizers asymptotically tends to a Gaussian distribution with mean $\mu_i = Mp_i$ and variance $\sigma_i^2 = Mp_i(1-p_i)$ [3]. Then, the decision threshold λ is chosen as two Gaussian distributions that are equal, i.e.,

$$\frac{1}{\sqrt{2\pi\sigma_1^2}}\exp\left[-\frac{(\lambda-\mu_1)^2}{2\sigma_1^2}\right] = \frac{1}{\sqrt{2\pi\sigma_2^2}}\exp\left[-\frac{(\lambda-\mu_2)^2}{2\sigma_2^2}\right]. \quad (2)$$

The decoded binary digits 0 and 1 are then obtained from $y < \lambda$ and $y \geq \lambda$, respectively. Compared with the digital source, the probability of error P_e is obtained. In Fig. 2a, for the input signal-to-noise ratio (SNR) $10\log(A/\sigma_\xi) = 1.46$ dB, P_e is plotted versus the added noise level σ_η of Gaussian noise η_m for a different number of M sensors. As the added noise level σ_η increases, P_e first decreases, and then reaches a minimum at an optimal level σ_η, and finally increases for very large noise levels σ_η. Moreover, as the number of quantizers M increases, the minimum of P_e can gradually decrease. This is the stochastic resonance effect in quantizer arrays.

Interestingly, for a large number of M sensors (e.g., $M = 10^4$), the minimum P_e manifests over a wide range of added noise level of $\sigma_\eta \in [0.8,10]$. This robust feature facilitates the incorporation of the added noise into the signal detection without finding the optimal noise level. For a technological application, for instance, a long-span bridge may need thousands of sensors for continuous monitoring of its structural state, and those sensors also endure strong ambient noise that stems from wind or car tires. An experimental investigation has been carried out with a low-grade iPhone accelerometer to extract the first four fundamental frequencies of a highway bridge [7]. A parallel array of such sensors distributed over a long-span bridge could possibly benefit from the ambient noise for detecting structural conditions of the bridge. Another technological application is the addition of noise to the image sensor unit of 10 × 10 photodetectors that can widen the response region and let the system respond to strong light [10]. Similar exploitation of the background noise is potentially accessible

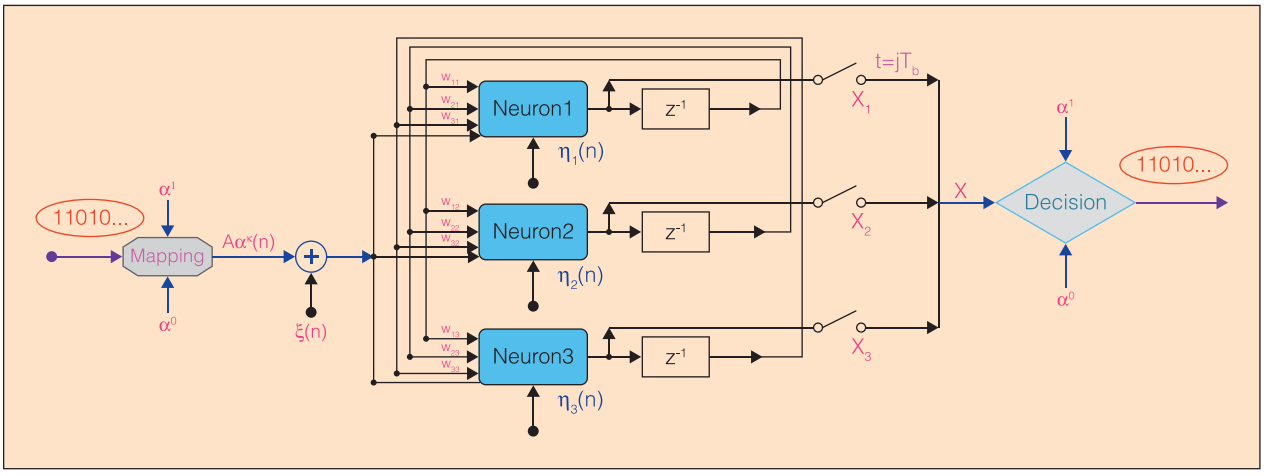

Fig. 3. Binary signal transmission in a discrete Hopfield network with $M = 3$ neurons.

for data processing from large numbers of low-cost sensors in sensor-swarm or sensor-cloud applications.

For detecting a known signal in additive white Gaussian noise, the optimal detector rests on a linear test statistic known as the matched filter or correlation receiver [1], [3], [9]. This linearity entails simplicity for both practical implementation and theoretical analysis, and as a result, the matched filter is very often exploited for detection, even when it is, strictly, no longer optimal for detecting known signals in non-Gaussian noise. For these reasons, the matched filter represents a meaningful reference that we shall use for comparison with our quantizer arrays. For detecting the binary pulse-amplitude modulated waveforms $s_i(n) = \pm A$ in the noisy input $x(n)$ over a time interval $n_0 \le n \le n_0 + N$ (N is an integer), the matched filter utilizes the test statistic:

$$\sum_{n=1}^{N} s_1(n)x(n) \ge 0 \tag{3}$$

to accept the hypothesis $s_1(n) = +A$ (digit 1), and otherwise $s_0(n) = -A$ (digit 0) with the decision threshold of zero. The probability of error of matched filter [1], [3], [9] can be computed as:

$$P_e = \int_{\sqrt{NA^2/\sigma_\xi^2}}^{+\infty} \frac{1}{\sqrt{2\pi}} \exp\left(-\frac{t^2}{2}\right) dt. \tag{4}$$

For instance, at a fixed added noise level $\sigma_\eta/\gamma = 1$ and for the quantizer array size $M = 10^3$, the probability of error P_e is plotted as a function of input SNRs in Fig. 2b. For comparison, the probability of error P_e of the matched filter in (4) is also plotted for $N = 1$. For low input SNRs, the noise-enhanced quantizer array performs as well as the matched filter.

From Parallel Array of Sensors to Hopfield Networks

Recent results provide insight into the noise benefit to the functional organization of complex neural or communication networks [8]–[11]. To illustrate the behavior of a Hopfield network for transmitting binary signals, an architectural graph of $M = 3$ neurons is shown in Fig. 3. The discrete Hopfield neural network has two M-dimensional fundamental memory vectors α^κ ($\kappa = 0,1$). The binary digits 0 and 1 map onto vectors α^0 and α^1, respectively. The modulated amplitude is A and the bit duration is T_b. Then, the modulated vectors $A\alpha^\kappa(n)$ are corrupted by the background noise vector $\xi(n)$, yielding the input vector of the network as:

$$\boldsymbol{S}^\kappa(n) = A\boldsymbol{\alpha}^\kappa(n) + \boldsymbol{\xi}(n). \tag{5}$$

Each element $S_m^\kappa(n)$ is fed into the m-th neuron with its activity function φ and output:

$$x_m(n+1) = \varphi\left(\sum_{i=1}^{M} w_{im}x_m(n) + S_m^\kappa(n) + \eta_m(n)\right), \tag{6}$$

where the synaptic weight from neuron i to neuron m is w_{im} and the added noise components are $\eta_m(n)$. We can combine these synaptic weights w_{im} as the M-by-M matrix form:

$$\boldsymbol{W} = \frac{1}{2}\sum_{\kappa=0}^{1} \boldsymbol{\alpha}^\kappa \left(\boldsymbol{\alpha}^\kappa\right)^T \tag{7}$$

according to Hebb's rule of the outer product [11]. At sampling times n, the outputs $x_m(n)$ comprise the network output state vector $\boldsymbol{X}(n)$, as shown in Fig. 3. We define the potential energy function as:

$$E(n) = \frac{1}{2}\boldsymbol{X}^T(n)\boldsymbol{W}\boldsymbol{X}(n) - \sum_{m=1}^{M}\int \varphi\left(\sum_{i=1}^{M} w_{im}x_m(n) + A\alpha_m^\kappa(n)\right) dx_m, \tag{8}$$

which has one global minimum but multiple possible local minima at stable vectors $\boldsymbol{X}^* = \varphi(\boldsymbol{W}\boldsymbol{X}^* + A\alpha^\kappa)$. For a not too short bit duration T_b, we expect that the state vector $\boldsymbol{X}(T_b)$ converges

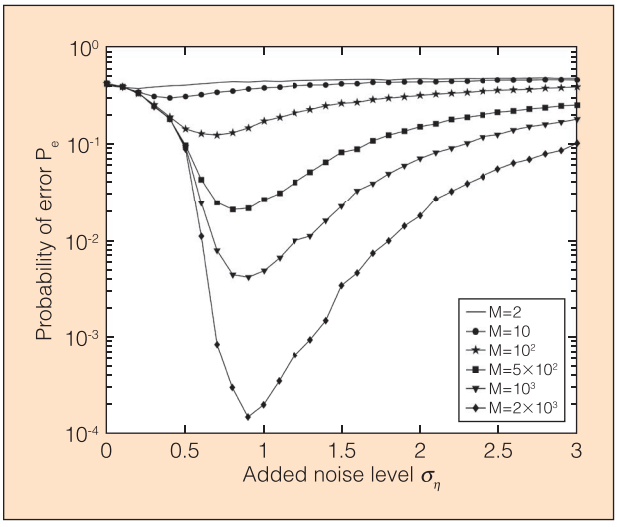

Fig. 4. Probability of error P_e versus added noise level σ_η for Hopfield networks with M neurons.

to the designed stable vector $\boldsymbol{X}^\kappa$ that are very close to but not simply identical to the stored memory vector α^κ. Then, at sampling times $n = jT_b$ for $j = 1,2,\ldots$, we compute the scalar inner products $\boldsymbol{X}^T(jT_b)\alpha^1 \geq \boldsymbol{X}^T(jT_b)\alpha^0$ to decode the network output as the digit 1 and otherwise the digit 0, where $\boldsymbol{X}^T(jT_b)\alpha^\kappa$ is also called the overlap between $\boldsymbol{X}(jT_b)$ and α^κ.

When comparing the decoded digits with the original digits, the probability of error P_e is plotted as a function of added noise level σ_η for different numbers of neurons in the Hopfield network, as shown in Fig. 4. Due to the weak amplitude of the vector $A\alpha^\kappa(n)$, the state vector $\boldsymbol{X}(n)$, assistance from the noise, switches correctly to follow the variability of the binary information carried in each of the successive time intervals T_b. As a result, a high probability of detection error P_e ensues, which is gradually reduced as the noise level σ_η rises above zero, with a more pronounced improvement for larger array sizes M, and with an optimal non-zero amount of noise maximizing the benefit. Here, the modulated amplitude $A/\sigma_\xi = 1$, the bit duration $T_b = 3$ and the activity functions $\varphi(\cdot) = \tanh[\beta(\cdot)]$ with the

Table 1 – Vibration levels of micro-motors versus driving voltages

Voltages (V)	0	0.6	1.4	1.8	2.2	2.9
Levels	0	1	2	3	4	5

slope parameters $\beta = 1.2$. Both background noise $\xi(n)$ and the added noise $\eta_m(n)$ are Gaussian distributed. As the number of neurons M increases, the probability of error P_e gradually drops to a valley, reaches the valley bottom at an optimal interval noise level σ_η, and finally climbs out of the valley for large noise levels σ_η. The noise benefit to the binary signal transmission is also evident in the Hopfield network. We emphasize that the noise-induced effect in Hopfield networks occurs in a multi-dimensional vector space $\{\alpha^\kappa\}$, which greatly extends two unidimensional states of quantizers in sensor arrays. At an optimal noise level σ_η, the network state vector $\boldsymbol{X}(n)$, assisted by internal noise, will capture the variability of input binary modulated vectors more correctly. It can be noted that information is carried here in the instant values of the input signal visiting the two patterns α^0 and α^1 but not in the memory contained in the temporal sequencing of these values. In addition, the binary signal transmission scheme can be extended to the M-ary signal case, wherein the multiple stored patterns α^κ represent M-ary digits.

From Neural Networks to Human Hand Balance

Noise or vibration plays a positive role not only in the detectability of the sensor arrays and networks [1]–[10], but also in the sensitivity of medical and biological systems [11]–[14]. Mechanical and electrical noise has been shown as beneficial to human sensory systems [11]–[14].

High-frequency sinusoidal interference can be viewed as a special kind of noise [9], [14]. This inspires us to exploit the effects of mechanical vibration of micro-motors on the balance control of human hands, as illustrated in Fig. 5. The reason is that the cutaneous mechanoreceptors reach a perception

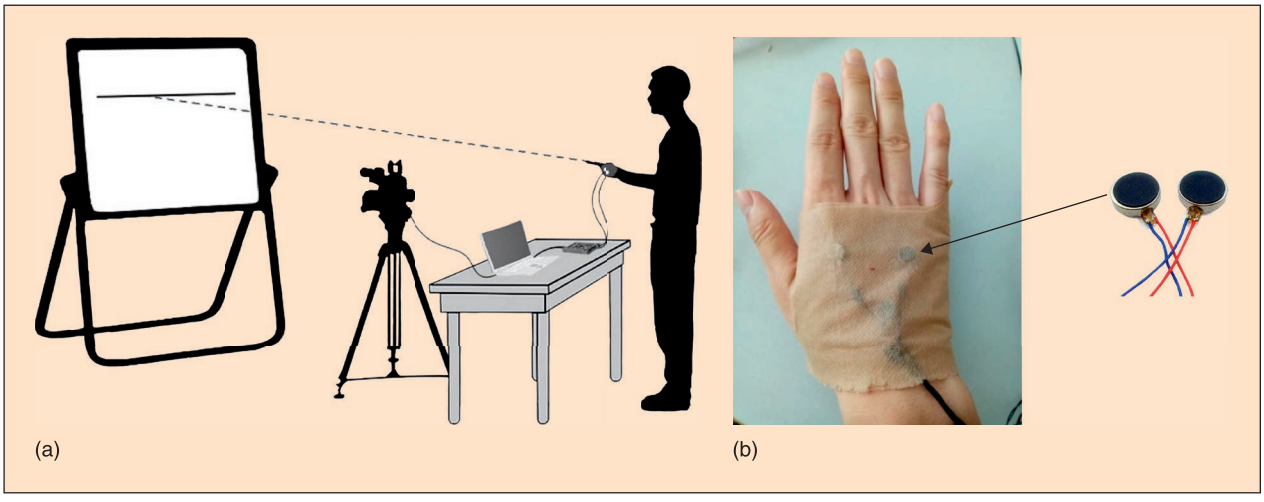

Fig. 5. (a) A subject grasping a laser pointer to draw a line on the whiteboard; (b) Opisthenar of the subject stimulated by micro-motors (8 mm diameter and 3.5mm thickness).

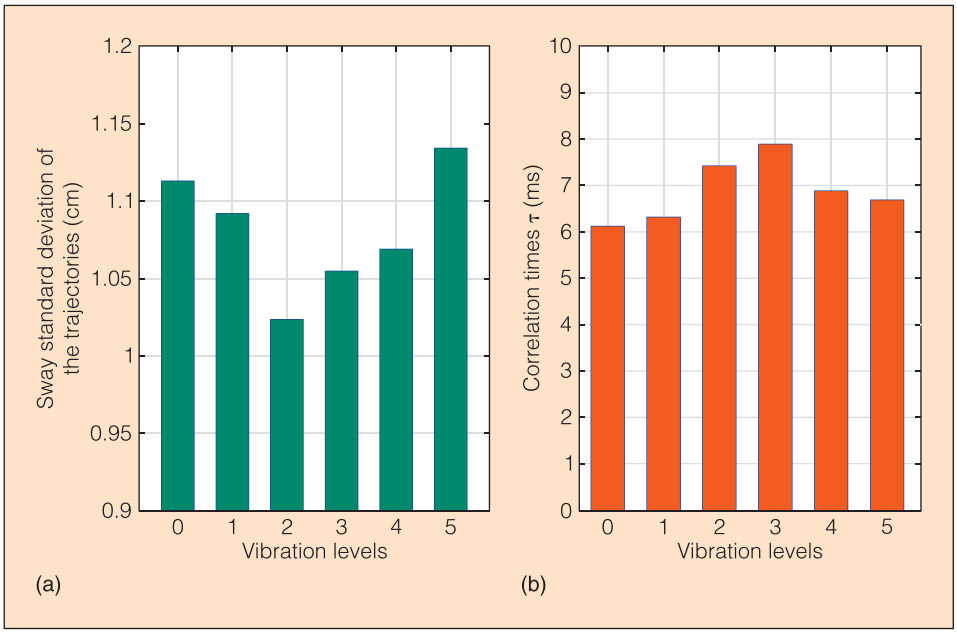

Fig. 6. (a) Sway standard deviations and (b) correlation times of the trajectories of the laser pointer versus vibration levels of micro-motors.

threshold, and that situation mimics the McCulloch-Pitts neuron model to the central nervous system for information processing. Each motor is driven by the microcontroller STM-32F103ZET6 [14], and several micro-motors, tied by nonwoven fabric, are applied on the cutaneous mechanoreceptors of the opisthenar. The integrated development environment is KEIL-MDK ver. 5.0, and the micro-motors, of reference CO834B002F, has a rated speed 9000 ~ 15000 rad/min and a rated current 100 mA. The microcontroller has 4 channel outputs of the pulse width modulation to control the electric voltage of micro-motors [14]. Vibration interference amplitudes that are proportional to the driving voltage are listed in Table 1. For instance, the zero level implies no driving voltage, and level 1 is at the perception threshold. Wearing vibration micro-motors operated at different levels, subjects draw a line on the white-board, which is recorded and processed by the Video-Capture class of the OpenCV software at the rate 25 (fps) of frame capture. At sampling times $n\Delta t$ for $n = 0,1,2,\ldots$, the recoded images provide the trajectory ordinates by the Simple-Blob detector, yielding the sequence of the trajectory $x(n)$. Each trial takes 20-30 s, during which the upper arm of the subject does not rest on the body [14].

After 30 trials for six subjects, the average sway standard deviation at each vibration level is illustrated in Fig. 6a. The sway standard deviation of the laser pointer within the subject's hand is smallest at the vibration level 2. In order to measure the relation between different times, we also approximately compute the autocorrelation function of the trajectory $x(n)$ of the laser pointer as:

$$R(n) = \frac{1}{N-m}\sum_{n=1}^{N-m} x(n)\,x(n+m), \tag{9}$$

and define the correlation time $\tau = n_0\Delta t$ as:

$$R(\tau) \le 0.05R(0) \tag{10}$$

with the sampling time Δt = 0.04s. As indicated in Fig. 6b, at the vibration levels 2-3, the correlation time τ is much higher than that obtained by other levels, which indicates more coherence of hand movements in the interval of correlation time τ. These results imply that vibration has the potential for hand balance control and might provide a noninvasive method for the sensitivity improvement of the human hand for daily living tasks.

Summary

In this article, the constructive role of noise in sensors is presented. From an individual sensor to an array of sensors, it is found that the noise benefits get enhanced as the array size increases. Moreover, for a representative Hopfield network, the switch between multi-dimensional state vectors can be assisted by a suitable amount of neuronal noise, yielding lower error-probability transmission for binary signals. Furthermore, we attach vibrating micro-motors on human hands and find an optimal vibration level that enhances the sensitivity of hand movements. Since noise is inevitable in sensors or neurons, some interesting structures can be devised by exploiting noise in nonlinear sensors.

References

[1] M. D. McDonnell and D. Abbott, "What is stochastic resonance? definitions, misconceptions, debates, and its relevance to biology," *PLOS Computational Biology*, vol. 5, art. no. e1000348, 2009.

[2] L. Gammaitoni and A.R. Bulsara, "Noise activated nonlinear dynamic sensors," *Physical Review Letters*, vol. 88, art.no. 230601, 2002.

[3] M. D. McDonnell, N. G. Stocks, C. E. M. Pearce, and D. Abbott, *Stochastic Resonance: From Suprathreshold Stochastic Resonance to Stochastic Signal Quantization*. New York, NY, USA: Cambridge University Press, 2008.

[4] B. Andò, "Noise and visual perception," *IEEE Instrum. Meas. Mag.*, vol. 15, pp. 45-48, 2012.

[5] B. Andò, S. Graziani, and N. Pitrone, "Characterization of threshold-induced phenomena deterministic driven devices," *IEEE Trans. Instrum. Meas.*, vol. 54, pp.1045-1053, 2005.

[6] A. R. Bulsara, "No-nuisance noise," *Nature*, vol. 437, pp. 962-963, 2005.

[7] A. Elhattab, N. Uddin, and E. OBrien, "Extraction of bridge fundamental frequencies utilizing a smartphone MEMS accelerometer," *Sensors*, vol. 19, art. no. 3143, 2019.
[8] M. E. Inchiosa and A. R. Bulsara, "Coupling enhances stochastic resonance in nonlinear dynamic elements driven by a sinusoid plus noise," *Physics Letters A*, vol. 200, pp. 283-288, 1995.
[9] Y. Ren, Y. Pan, F. Duan, F. Chapeau-Blondeau, and D. Abbott, "Exploiting vibrational resonance in weak-signal detection," *Physical Review E*, vol. 96, art.no. 022141, 2017.
[10] Y. Tadokoro, S. Kasai, A. Ichiki, and H. Tanaka, "Design framework of image sensor system based on dynamic range extension by adding noise for saturated conditions," *IEEE Trans. Syst., Man, and Cybernetics: Syst*., vol. 46, pp. 1121-1128, 2016.
[11] N. Katada and H. Nishimura, "Stochastic resonance in recurrent neural network with Hopfield-type memory," *Neural Processing Letters*, vol. 30, pp. 145-154, 2009.
[12] J. J. Collins, A. A. Prilata, D. C. Gravelle, J. Niemi, J. Harry, and L. A. Lipsitz, "Noise-enhanced human sensorimotor function," *IEEE Eng. in Medicine and Biology Mag*., vol. 22, pp. 76-83, 2003.
[13] E. A. Keshner, J. C. Slaboda, L. L. Day, and K. Darvish, "Visual conflict and cognitive load modify postural responses to vibrotactile noise," *J. Neuro Engineering and Rehabilitation*, vol. 11, pp.1-9, 2014.
[14] L. Zhang, H. Sun, Y. Pan, and F. Duan, "Experimental study of vibration resonance aided systems in human hand movement," *Complex Syst. and Complexity Science*, vol. 14, pp. 72-78, 2017.

Fabing Duan (fabing.duan@hotmail.com) is currently a Professor of System Science at Qingdao University, China. He received the Master's degree in engineering mechanics from the China University of Mining and Technology, Beijing in 1999. He received the Ph.D. degree in solid mechanics at Zhejiang University, China in 2002. From 2002 to 2003, he was a postdoctoral fellow at the University of Angers, France. Since 2004, he has been with the Institute of Complexity Science, Qingdao University, China. His research interests are in nonlinear systems and signal processing.

Lingling Duan is currently working toward the Ph.D. degree in system science at Qingdao University, China. She received the Master's degree in computational mathematics at Xiamen University, China, in 2008. Her research interest is noise-enhancement effects in neural networks.

François Chapeau-Blondeau (chapeau@univ-angers.fr) is currently a Professor of Electrical and Electronic Engineering with the University of Angers, France. He received the Engineer Diploma from ESEO, Angers, France in 1982, and the Ph.D. degree in electrical engineering from University Pierre & Marie Curie, Paris 6, France in 1987. His research interests include information theory, signal processing and imaging, and the interactions between physics and information sciences.

Yuhao Ren has been a lecturer at Qingdao University, China since 2018, when he received the Ph.D. degree in system science. His research interest is vibrational resonance effects and nonlinear signal processing.

Derek Abbott (M'85–SM'99–F'05) (derek.abbott@adelaide.edu.au) has been with The University of Adelaide, SA, Australia since 1987, where he is currently a full Professor with the School of Electrical and Electronic Engineering. He received the B.Sc. degree in physics from Loughborough University, Leicestershire, U.K. in 1982 and the Ph.D. degree in electrical and electronic engineering from The University of Adelaide, SA, Australia in 1995. His research interests include multidisciplinary physics and electronic engineering applied to complex systems, networks, game theory, energy policy, stochastics, and biophotonics.